Identification of Benign and Malignant Tumor from Chest CT Scans By Using Support Vector Machine

Ganesh Sable1, Harsha Bodhey2

1Professor, Savitribai Phule Women's Engineering College, Aurangabad, Maharashtra, India
sable.eesa@gmail.com
2Student, Savitribai Phule Women's Engineering College, Aurangabad, Maharashtra, India
harsha.bodhey@gmail.com

Abstract: Lung cancer is the number one cause of death every year and is the second most diagnosed after the breast and prostate cancer in women and men respectively. Nowadays, the lung lobe segmentation is the most basic step in early diagnosis of lung diseases and the analysis of pulmonary functions. Segmentation of the lobes is relevant in clinical practice. This paper aims at developing an efficient and cost effective system for lung segmentation and tumor identification from CT scan images. In pre-processing, first input image is converted into gray scale image and then wiener filter of mask 3*3 is used for removing noise present in the image. In post-processing, lungs and lobes segmentation and tumor classification is done. At last, the tumor present in the image is segmented. Lung segmentation is done by using adaptive thresholding. Marker based watershed transformation is used for lobe segmentation. Then, some important textural features of each image are extracted using GLCM. After this step, a supervised learning model i. e. SVM is used for the identification of benign and malignant tumor. After classification, the tumor presented in the input image is segmented using FCM algorithm. The required database contains 51 lung CT scans and is taken from LOLA 11 segmentation challenge. The proposed system is implemented in Matlab/R2012a software and has achieved an average accuracy of 95.56%.

Keywords: Lung Segmentation, Watershed Transformation, Feature Extraction, GLCM (Gray Level Co-occurrence Matrix), FCM (Fuzzy C-means), SVM (Support Vector Machine).

1. Introduction

Today segmentation of images has become important and effective tool for many technological applications. Pulmonary CT scan images have an important role in the diagnosis of several lung diseases such as lung cancer, old or new pneumonia, tuberculosis, emphysema and chronic obstructive lung diseases (COPD) [1]. The lungs are divided into lobes, separated by a thin sheet of tissue, the fissures. The left lung has one oblique fissure and thus two lobes; the right lung has an oblique and a horizontal fissure, and thus three lobes. Lung and lobe segmentation is relevant in clinical applications particularly for treatment planning. The location and distribution of pulmonary diseases are important parameters for the selection of a suitable treatment. Many of the lung diseases affect the separate lung lobes to a different extent. Sometimes a disease may even be confined to a single lobe. Therefore lobe-by-lobe quantification of the lungs becomes important for disease severity estimation and treatment planning.

Tumor is a mass produced as a result of uncontrolled growth of the lung tissues. It is mainly classified as benign and malignant. Benign tumors are noncancerous cells, but if they can harm other tissues if not treated in time; while Malignant tumors are cancerous cells. CT is a nondestructive technique for visualizing interior features within solid objects, and for obtaining digital information on their 3-D geometries and properties.

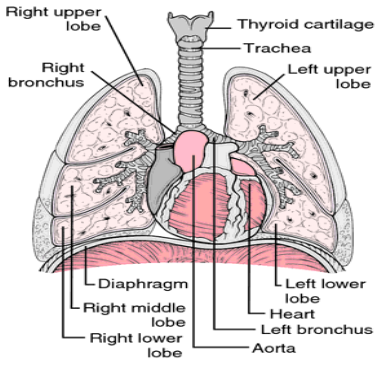

Figure 1: Lung anatomy

This imaging modality provides detailed cross sectional images of thin slices of the human body. CT datasets can contain over 1000 images, therefore manually segmenting the lungs is tedious and prone to inter observer variations. The nodules are situated within the lung parts of the CT scan image that is usually less than half of the area of CT slice. If nodules have to search in the whole slice, it will take a long time. To reduce time to search nodules in the CT slice, we have to search only in the area where the

nodule is present in the slice. Therefore a mechanism is needed to segment that part of the lung. Automated segmentation of anatomical structures is challenging in cases with abnormalities. Thus we have proposed a new approach for lung segmentation and tumor identification from CT scan images and tried to overcome the above drawbacks.

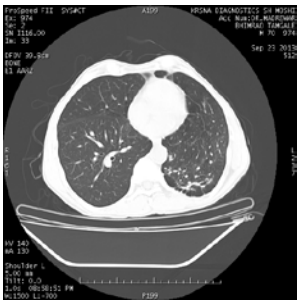

Figure 2: Original lung CT image

2. Existing systems

Many authors explored the segmentation techniques in medical imaging depending on the region of interest till now [3]. Some of them use a semi-automatic algorithm and still need some user interaction, while others are fully automatic and the user has only a verification role. Various algorithms from different authors can be found for medical image segmentation such as region growing [2], thresholding [4]. A. Hoffman [5] have developed an automatic method for identifying lungs in 3D X-ray CT images. Zhang and Valentino [7] have suggested using artificial neural networks to classify each pixel in the CT slice into different anatomical structure. Sluimer et. al. [11] used the boundary curvature to estimate in a wide variety of image segmentation and analysis. Mithun N. et. al. [12] used an adaptive thresholding method which performs the segmentation of the lungs by comparing the curvature of the lung boundary to that of the ribs. This technique improves the fixed threshold based approaches to include lung boundary curvature features. Some authors have proposed systems for lung tumor classification from CT scan images using ANN [13], segmentation fuzzy system [14]. Some authors have proposed systems for nodule detection and classification using FIS [19], neural network [20], Bayesian classifier [21], neuro fuzzy logic [22]. They all have tried to increase the accuracy of tumor classification. Here, we have proposed a novel approach for lung segmentation and tumor identification from CT scans and tried to improve the accuracy as compared to existing systems.

3. Proposed method

3.1 Introduction

Here, a new system is proposed for lung segmentation and tumor classification from CT scan images.

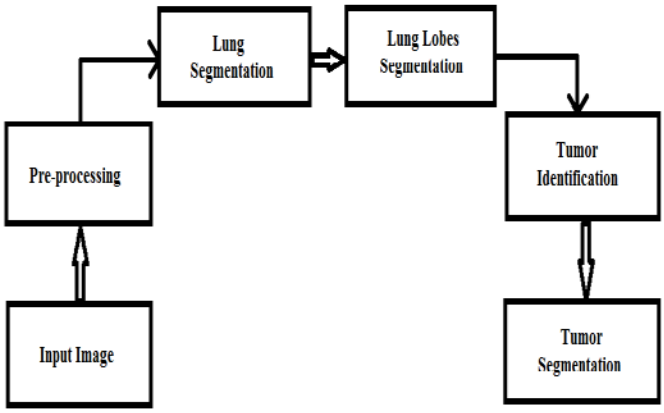

Figure 3: Block diagram of the lung tumor identification system

Above figure 3 shows the block diagram of the proposed lung tumor identification system. It consists of the following steps.

3.2 Pre-processing

Pre-processing includes following steps:

i. Input image

Here, the input images are chest CT scan images in JPEG format that contain tumors. First image selected from the file specified by the string filename. The user has to select the required lung CT scan image for further processing. Then each image is resized to 256*256.

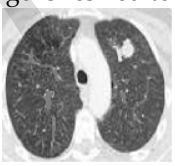

Figure 4: Input image

ii. Wiener filtering

The input image is in RGB format. So it is first converted into gray scale image; since most of the image processing is done on gray scale images. Generally, medical images are corrupted with noise and artefacts due to body movements. Thus wiener filter of mask size 3*3 is used to remove noise because it is one of the efficient methods to remove the noise from the CT images [21].

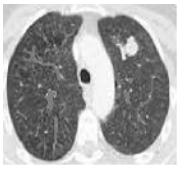

Figure 5: Filtered image

3.3 Post processing

the GLCM to the GLCM diagonal.

Post-processing includes following steps:

i. Lung segmentation:

Image segmentation is the process of assigning a label to every pixel in an image such that pixels with the same label share certain visual characteristics. In this step, we have segmented left and right lung from the CT image. First we have chosen the seed point in the CT image. From the point we found intensity value of the image. We compare the intensity value between the neighboring pixels and current pixel. If the neighbor pixels values are related to the seed value, it will segment lungs from the original image. These similarity pixels will be segmented from the CT image []. This process is continued until reach the last pixel. Finally the lungs will be segmented. Threshold value between 0 and 180 is selected. Along with this some morphological operations like opening, closing, erosion, hole filling are also used for lung segmentation.

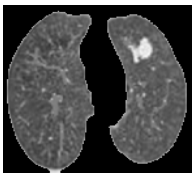

Figure 6: Lung segmentation

ii. Lobe segmentation:

Watershed transformation is a common technique for image segmentation. However, its use for automatic medical image segmentation has been limited particularly due to over segmentation and sensitivity to noise [16]. Employing prior shape knowledge has demonstrated robust improvements to medical image segmentation algorithms. We propose a novel method for enhancing watershed segmentation by utilizing prior shape and appearance knowledge. Each region defined by the external markers contains a single internal marker and part of the background.

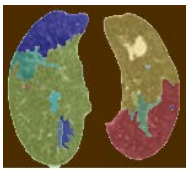

Figure 7: Lobe segmentation

iii. Feature extraction:

Texture feature have been widely used to classify normal and abnormal pattern in digital images. In this step, total 12 textural features of all images in the database are extracted using GLCM (Gray level co-occurrence matrix). These features are used for tumor classification.

GLCM is simply a matrix that gives the sum of the number of times that the pixel with value *i* occurred in the specified spatial relationship to a pixel with value *j* in the input image. Texture feature calculations use the contents of the GLCM to give a measure of the variation in intensity at the pixel of interest. These GLCM features calculated for some of the images are shown in following table:

Table 1: GLCM features and their values

GLCM features	Image 1	Image2
autoc	32.9612	39.6644
contr	0.3473	0.3034
corrm	0.9726	0.9520
corrp	0.9726	0.9520
cprom	739.3252	177.3976
cshad	-5.9851	3.7745
dissi	0.2396	0.2379
energy	0.1737	0.2551
entro	2.1526	1.7496
homom	0.8943	0.8909
homop	0.8903	0.8876
maxpr	0.2924	0.4250

Like this, these GLCM features are calculated for all images in database.

GLCM features:

1. autoc (Autocorrelation): It is used for finding repeating patterns in an image.

$$\sum_{i=0}^{G-1}\sum_{j=0}^{G-1}(p_x-\mu_x)(p_y-\mu_y)/\sigma_x\sigma_y$$

	1
1	32.9612
2	39.6644
3	27.5840
4	29.7253
5	28.6981
6	30.9689

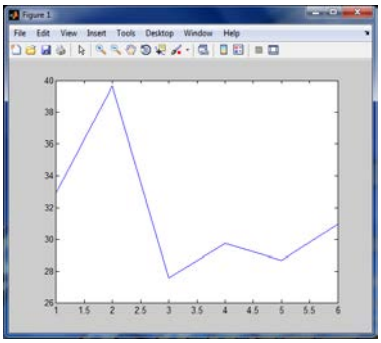

Figure 8: Values and graph of autocorrelation

2. Contr (Contrast): It is a measure of the intensity contrast between a pixel and its neighbor over the whole image.

$$\sum_{i,j=0}^{G-1}(i-j)^2P(i,j)$$

2
0.3473
0.3034
0.4056
0.4348
0.3787
0.5062

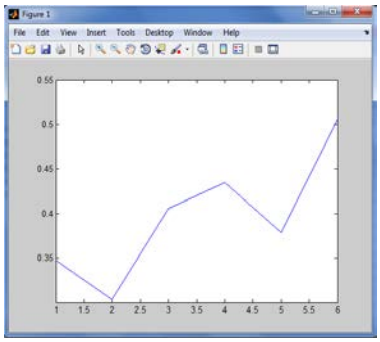

Fogure 9: Values and graph of contrast

3. corr (Correlation): It is a measure of gray level linear dependence between the pixels at the specified positions relative to each other.

$$\sum_{i=0}^{G-1}\sum_{j=0}^{G-1}\frac{\{i\times j\}\times P(i,j)-\{\mu_x\times\mu_y\}}{\sigma_x\times\sigma_y}$$

3
0.9726
0.9520
0.9754
0.9473
0.9649
0.9295

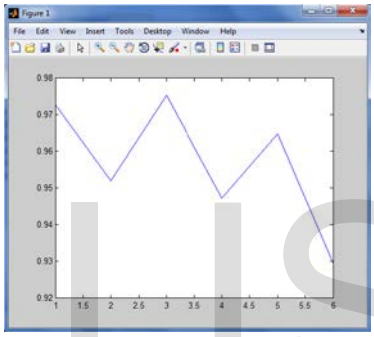

Figure 10: Values and graph of correlation

4. cprom (Cluster prominence): It gives the measure of the degree to which the outliers in the histogram favor one side or another of the statistical mean.

$$\sum_{i=0}^{G-1}\sum_{j=0}^{G-1}\{i+j-\mu_x-\mu_y\}^4\times P(i,j)$$

5
739.3252
177.3976
1.3306e+03
341.4651
657.9697
246.5660

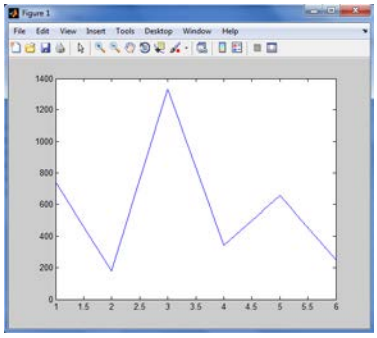

Figure 11: Values and graph of cluster prominence

5. cshad (Cluster shade): It is a measure of skewness of the matrix.

$$\sum_{i,j=0}^{G-1}(i+j-\sigma_I-\sigma_J)^3P(i,j)$$

6
-5.9851
3.7745
62.2282
17.9525
-8.5273
-6.6419

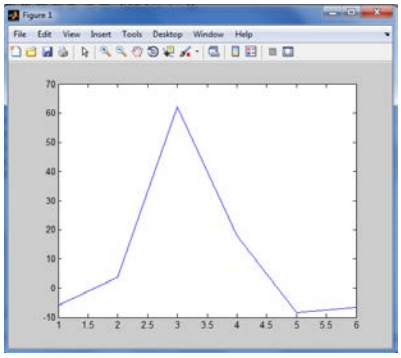

Figure 12: Values and graph of cluster shade

6. dissi (Dissimilarity): It gives the measure of much dissimilar are of two neighboring pixels.

$$\sum_{i,j=0}^{N-1}P_{i,j}\left|i-j\right|$$

7
0.2396
0.2379
0.2142
0.3075
0.2283
0.2923

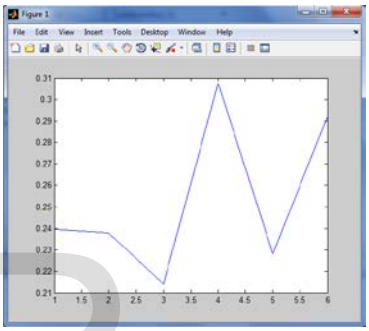

Figure 13: Value and graph of dissimilarity

7. energ (Energy):

It is also known as uniformity of ASM (angular second moment) which is the sum of squared elements from the GLCM.

Range = [0 1] Energy is 1 for a constant image.

$$\sum_{i,j=0}^{G-1}P(i,j)\,2$$

8
0.1737
0.2551
0.2675
0.1695
0.2156
0.2070

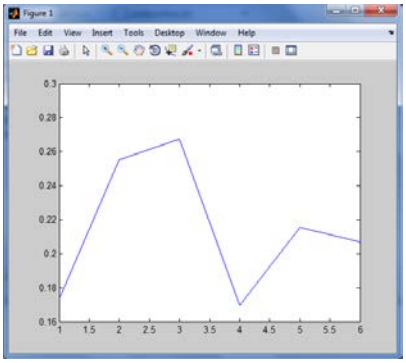

Figure 14: Values and graph of energy

8. entro (Entropy):

It is a measure of randomness. Entropy measures the loss of information or message in a transmitted signal and also measures the image information.

$$-\sum_{i=0}^{G-1} p(z_i)\log_2 p(z_i)$$

9
2.1526
1.7496
1.8898
2.2223
2.0985
2.1386

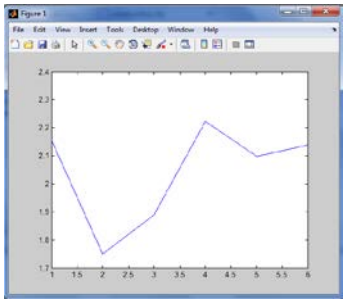

Figure 15: Values and graph of entropy

9. homom (Homogeneity):

It returns a value that measures the closeness of the distribution of elements in

$$\sum_{i=0}^{G-1}\sum_{j=0}^{G-1}\frac{1}{1+(i-j)^2}P(i,j)$$

10
0.8943
0.8909
0.9169
0.8646
0.9062
0.8821

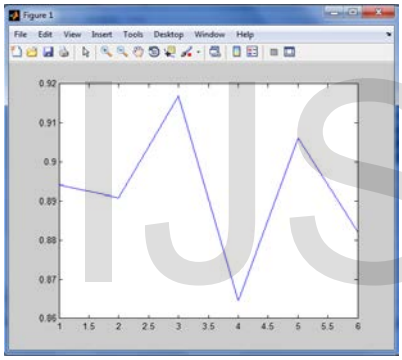

Figure 16: Values and graph of homogeneity

10. maxpr (Maximum probability):

This simple statistic records in the centre pixel of the window the largest P_{ij} value found within the window.

Max (i,j) P(i,j)

12
0.2924
0.4250
0.3739
0.2886
0.3385
0.3206

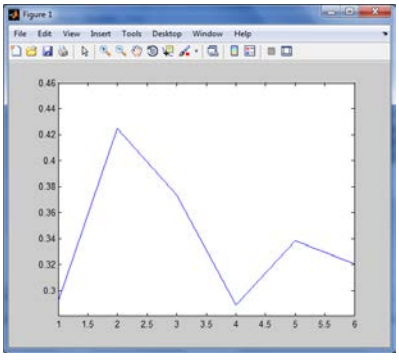

Figure 17: Values and graph of maximum probability

3.4 Tumor classification

After extracting GLCM features of images, tumor classification is done. For this, we have used SVM (Support vector machine) classifier. This classifier is trained first. Here, two class SVM classifier is used. An SVM classifies data by finding the best hyperplane that separates all data points of one class from those of the other class. The best hyperplane for an SVM means the one with the largest margin between the two classes. Margin means the maximal width of the slab parallel to the hyperplane that has no interior data points. The hyperplane is defined by the equation:

$$(w.x) + b = 0$$

Where, w= weight vector

x= feature vector

B= bias

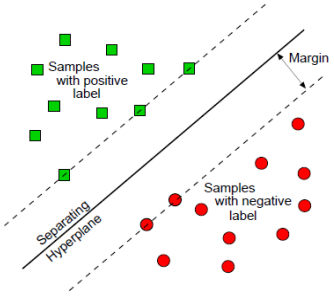

Figure 18: SVM classifier

The vectors closest to the boundaries are called support vectors and the distance between the support vectors and hyper plane is called margin [8]. SVM first maps the input feature vectors into higher dimensional feature space and then perform classification.

1. Training the classifier

In the training phase, known data is given and the classifier is trained. Here, six images are used for training out of which 3 are benign and 3 are malignant and are assigned class 0 for benign and class 1 for malignant. The training points satisfy the following conditions.

$(w.x_i) + b \geq +1$ for $y_i = +1$

$(w.x_i) + b \leq -1$ for $y_i = -1$

After training the classifier for proposed system, we got the value of bias -0.3481.

2. Testing of data

In testing phase, unknown data are given and the classification is performed using trained classifier. Classification is done by using following decision function.

$$f(x, \{w, b\}) = \text{sign}(w.x+b)$$

The sign of this function decides the class of the test image. Here, if it is positive, then result will be 'malignant' and if it is negative, then result will be 'benign'.

3.5 Tumor segmentation

Clustering is a process for classifying objects or patterns in such a way that samples of the same group are more similar to one another than samples belonging to different groups. Here fuzzy C-means algorithm is used for tumor segmentation from segmented lungs. Fuzzy clustering is basically a multi valued logic that allows intermediate values i.e., member of one fuzzy set can also be member of other fuzzy sets in the same image. In the proposed FCM, The algorithm is an iterative clustering method that produces an optimal c partition by minimizing the weighted within group sum of squared error objective function J_{FCM} [6].

$$J_{FCM} = \sum_{k=1}^{n} \sum_{i=1}^{c} (u_{ik})^q \, d^2 (x_k, v_i) \quad \ldots\ldots(1)$$

The membership function defines the fuzziness of an image and also to define the information contained in the image. These are three main basic features involved in characterized by membership function. They are support, Boundary. The core is a fully member of the fuzzy set. The support is non membership value of the set and boundary is the intermediate or partial membership with value between 0 and 1. This clustering algorithm allows one piece of data may be member of more than one clusters. It is based on reducing the equation 2,

$$Y_m = \sum_{i=1}^{N} \sum_{j=1}^{C} M_{ij}^{m} \left\| x_i - c_j \right\|^2 \quad \ldots.(2)$$

Where,

m- Any real number greater than 1.

Mij- Degree of membership of X; in the cluster j

xi- Data measured in d-dimensional.

Cj - Dimension centre of the cluster.

‖Xi-Cj‖²- Induced norm (Euclidean norm)

This system uses two level segmentation i.e. for two levels of thresholding, image is divided into 3 clusters and maximum number of iterations is 100.

Figure 19: Tumor segmentation

3.6 System flowcharts

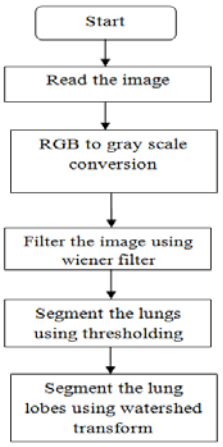

Figure 20: Flowchart for lobe segmentation

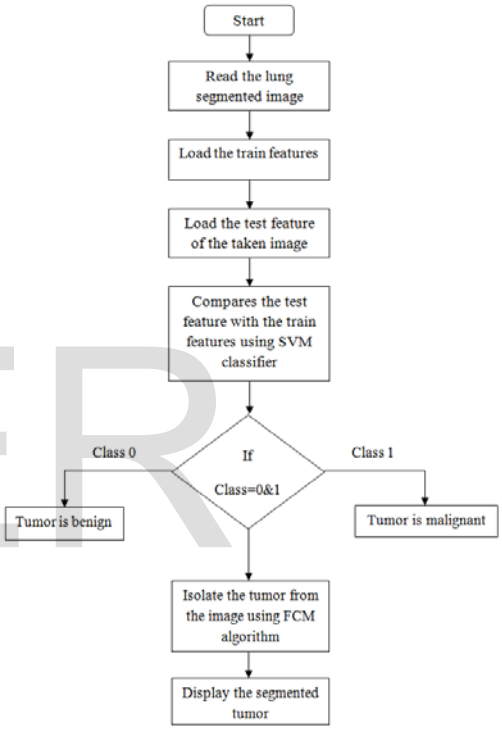

Figure 21: Flowchart for tumor classification and segmentation

3.7 Database

We have taken the database containing lung CT scans of 51 patients from Lola 11 segmentation challenge. All these images are of size 256*256 and are in JPEG format.

Some images from the database are shown in following figure:

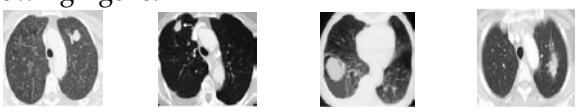

(a) (b) (c) (d)

Figure 22: Images from database

3.8 System requirements

1. Hardware specification

- Intel (R) Core i3 – 2.53 GHz
- 3GB RAM
- 250Gb Hard disk

2. Software specification

- Operating system : windows7
- Programing tool : Matlab 2012
- Version : 7.9

4. Experimental results

In this section, the results of the SVM classifier are shown for four images in the database.

Table 2: SVM outputs and accuracy parameters

Img No.	Expert's opinion	Experime-ntal results	SVM output	Parameter
1	Benign	Benign	Class 0	TP
2	Benign	Malignant	Class 1	FP
3	Malignant	Malignant	Class 1	TN
4	Malignant	Benign	Class 0	FN

Similarly, the results for all 51 images in the database are obtained.

Where,

TP- predicts benign as benign.

FP- predicts benign as malignant.

TN- predicts malignant as malignant.

FN- predicts malignant as benign.

When 45 test images were given to the system, we got

TP = 25

TN = 18

FP = 1

FN = 1

4.1 Performance measures

The following parameters are calculated on the basis of the results obtained for total 45 test images in the database out of 51.

1. Accuracy (AC) = (TP+TN) / (TP+TN+FP+FN)
= (25 + 18) / (45)
= 0.9556

Accuracy in % = 95.56%

2. Sensitivity (SE) = TP / (TP+FN)
= 25 / (25+ 1)
= 0.9615

Sensitivity in % = 96.15%

3. Specificity (SP) = TN / (TN+FP)
= 18 / (18 + 1)
= 0.9473

Specificity in % = 94.73%

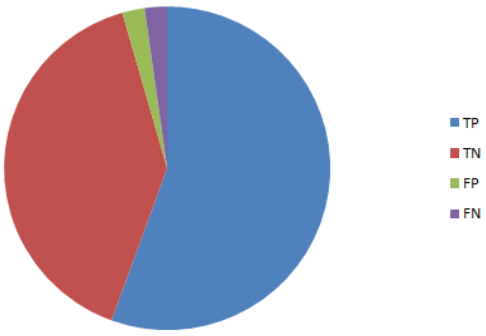

Graph 1: Accuracy parameters

From the above results it is found that our proposed system has achieved 95.56% accuracy, specificity of 94.73% and better sensitivity i.e. 96.15%.

4.2 Comparison with existing systems

Here, we have compared our proposed system performance with some of the existing systems as follows:

Ref. no.	Name of the author	Technology used	Accuracy
13	Yongjun WU, Na Wang, Hongsheng ZHANG, Lijuan Qin, Zhen YAN, Yiming WU	ANN	84.6%
14	S. Aravind Kumar, Dr. J. Ramesh, Dr. P. T. Vanathi and Dr. K. Gunavathi	Computer Aided Diagnosis, Segmentation Fuzzy Systems	90%
19	Atiyeh Hashemi, Abdol Hamid Pilevar, Reza Rafeh	Region growing algorithm and fuzzy interference system	95%
22	Varalakshmi.K	Neuro fuzzy system	89.3%
	Proposed system	GLCM and SVM	95.56%

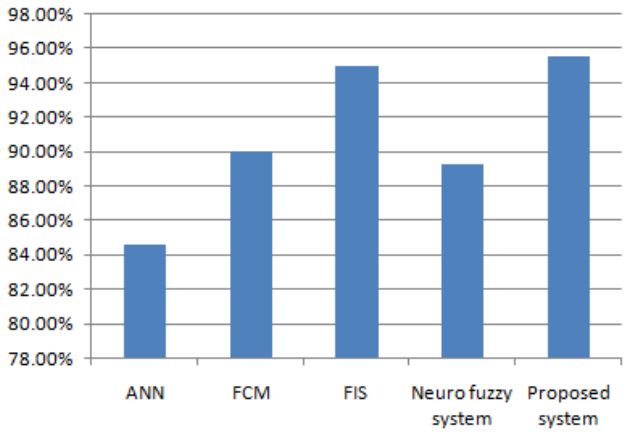

Graph 2: System comparison

5. Conclusions

A new system is developed for lung segmentation and tumor identification from chest CT scan images and is applied to 51 cases (256*256 pixel size). Out of 45 test images, 26 were benign and 19 were malignant tumors. The proposed system is able to detect both benign and malignant tumors more correctly. Thus from this and system comparison, it can be concluded that the SVM used for tumor classification has improved accuracy. Also the proposed method performs well and is robust against anatomical variations of the lungs. The system gives results within few seconds. Thus, this approach is a potential for developing an algorithm to segment lung, lobes and tumor identification for surgical planning of treating lung disease and it will assist radiologist as second opinion for the better diagnosis of lung cancer. The SVM classifier achieved an average accuracy of 95.56%.

6. Future scope

The automatic lobe segmentation and tumor classification has very wide scope since it reduces manual work and also computational time. Also it can be useful for diagnosis of other lung diseases. Further it can be performed for 3D images in future. The million order dataset can be selected and image classification can be done on larger dataset. With increased size of dataset various issues such as uploading data, managing feature set, increased execution time of classification algorithms etc. can be considered. More image features can be extracted for better classification. Various combinations of pre-existing features can be used to correctly classify medical data.

Acknowlegdement

I would like to express my gratitude with a word of thanks to my guide Mr. G. S. Sable sir for his valuable guidance and to all those who helped me in successfully completing my dissertation work.

References

[1] Bezdek J. C, "Pattern Recognition with Fuzzy Objective Function Algorithms", New York: Plenum Press, 1981.

[2] P. Croisille, M. Souto, M. Cova, S. Wood, Y. Afework, J. E. Kuhlman, E. A. Zerhouni, "Pulmonary nodules: improved detection with vascular segmentation and extraction with spiral CT", Radiology, Vol. 197, pp. 397-401, 1995

[3] D. L. Phan, C. Xu, J. Price, "A survey of current methods in medical image segmentation", Annual Review of Biomedical Engineering, 1998.

[4] Bezdek J. C, "Pattern Recognition with Fuzzy Objective Function Algorithms", New York: Plenum Press, 1981.

[5] P. Croisille, M. Souto, M. Cova, S. Wood, Y. Afework, J. E. Kuhlman, E. A. Zerhouni, "Pulmonary nodules: improved detection with vascular segmentation and extraction with spiral CT", Radiology, Vol. 197, pp. 397-401, 1995

[6] D. L. Phan, C. Xu, J. Price, "A survey of current methods in medical image segmentation", Annual Review of Biomedical Engineering, 1998.

[7] M. S. Brown, M. F. McNitt-Gray, J. G. Goldin, R. D. Suh, J. W. Sayre, D. R. Aberle, "Patient-specific models for lung nodule detection and surveillance in CT images", IEEE Transactions on Medical Imaging, Vol. 20, pp. 1242-1250, 2001.

[8] E. A. Hoffmann, J. M. Reinhardt, "Automatic Lung Segmentation for Accurate Quantitation of Volumetric X-Ray CT Images", IEEE Transactions on Medical Imaging, Vol. 20, pp. 490-498, 2001.

[9] B. Zhao, G. Gamsu and M. S. Ginsberg, "Automatic detection of small lung nodules utilizing local density maximum algorithm", Journal of Applied Medical Physics, vol.4, No.3, 2003.

[10] D. Zhang, D. J. Valentino, "Segmentation of anatomical structure in X-Ray computed tomography images using artificial neural network", Proc. of SPIE, vol. 4684, pp. 1640-1652, 2005.

[11] C. Sluimer, M. Prokop, and B. Van Ginneken, "Toward automated segmentation of the pathological lung in CT", IEEE Tran. on Medical Imaging, 24(8), pp 1025– 1038, 2005.

[12] Mithun N. Prasad, Matthew S. Brown, Shama Ahmad, Fereidoun Abtin, Jared Allen, Irene da Costa, Hyun J. Kim, Michael F. McNitt-Gray, Jonathan G. Goldin, "Automatic segmentation of lung parenchyma in the presence of diseases based on curvature of ribs", Academic Radiology, vol. 15, No 9, pp.1173-1180, September 2008

[13] Na Wang, H. Zhang, L. Qin, Z. Yan, and Y. Wu, "Application of Artificial Neural Networks in the Diagnosis of Lung Cancer by Computed Tomography", Sixth International Conference on Natural Computation, pp.147–153, 2010.

[14] S. Aravind Kumar, Dr. J. Ramesh, Dr. P. T. Vanathi, Dr. K. Gunavathi, "Robust and Automated Lung Nodule Diagnosis from CT Images Based On Fuzzy Systems", International Conference on Process Automation, Control and Computing (PACC), 2011.

[15] R. Nithya, B. Santhi, "Mammogram classification using maximum Difference feature selection method", Journal of Theoretical and Applied Information Technology, vol. 33, pp. 197-204, Nov. 2011.

[16] Nitish Zulpe, Vrushsen Pawar, "GLCM Textural Features for Brain Tumor Classification", International Journal of Computer Science Issues, Vol. 9, Issue 3, pp. 354-359, May 2012.

[17] M. Gomathi, Dr. P. Thangaraj, "An effective classification of benign and malignant nodules using support vector machine", Journal of Global Research in Computer Science, vol. 3, pp. 6-9, July 2012.

[18] Bianca Lassen, Eva M. van Rikxoort, Michael Schmidt, Sjoerd Kerkstra, Bram van Ginneken, and Jan-Martin Kuhnigk, "Automatic Segmentation of the Pulmonary Lobes From Chest CT Scans Based on Fissures, Vessels, and Bronchi", IEEE

Transactions on Medical Imaging, Vol. 32, No. 2, February 2013.

[19] Atiyeh Hashemi, Abdol Hamid Pilevar, Reza Rafeh, "Mass Detection in Lung CT Images Using Region Growing Segmentation and Decision Making Based on Fuzzy Inference System and Artificial Neural Network", International journal on Image, Graphics and Signal Processing, vol. 6, pp. 16-24, May 2013.

[20] Ada, Rajneet Kaur, "Early Detection and Prediction of Lung Cancer Survival using Neural Network Classifier", International journal of application or innovation in engineering and management, vol. 2, Issue 6, pp. 375-383, June 2013.

[21] T. Manikandan, D.Kesavaraja, "A study of different chest ct scan image segmentation for pulmonary lobes", International Journal of Research in Engineering & Advanced Technology, Vol. 1, Issue 5, pp. 1-8, Oct-Nov 2013.

[22] Varalakshmi.K, "Classification of Lung Cancer Nodules using a Hybrid Approach", Journal of Emerging Trends in Computing and Information Sciences, Vol. 4, pp. 63-68, Jan 2013.

[23] Anil M. Yametkar, R. D. Patane, "Lung Cancer Detection And Classification By Using Bayesian Classifier", Proceedings of IRF International Conference, Feb. 2014.

[24] S.Shaik Parveen, C.Kavitha, "Classification of Lung Cancer Nodules using SVM Kernels", International Journal of Computer Applications, Vol. 95– No.25, June 2014.

[25] R. C. Gonzalez, R. E. Woods, "Digital Image Processing", 3rd Edition, pp.738-756.